A new approach for measuring the carbon and oxygen content of atmospherically-relevant compounds and mixtures

James F. Hurley[1], Nathan M. Kreisberg[2], Braden Stump[3], Chenyang Bi[1], Purushottam Kumar[1], Susanne V. Hering[2], Pat Keady[3], Gabriel Isaacman-VanWertz[1]

[1] Department of Civil and Environmental Engineering, Virginia Tech, Blacksburg, VA, 24061
[2] Aerosol Dynamics Inc., Berkeley, CA, 94710
[3] Aerosol Devices Inc., Fort Collins, CO, 80524

Correspondence to: Gabriel Isaacman-VanWertz (ivw@vt.edu)

10 **Abstract**. While the mass of particulate matter is monitored worldwide, only a few automated approaches exist to characterize its composition in any detail. All approaches require relatively high capital costs and complex operation by highly trained technical personnel. This leaves a major gap in understanding the health and environmental impacts of particulate matter. In this work, we demonstrate a new approach to estimate the mass of carbon and oxygen in analytes and mixtures that relies only on robust, moderate cost detectors designed for use with gas chromatography. Organic compounds
15 entering a flame ionization detector were found to be converted with 95% efficiency to CO_2, which was analysed downstream using an infrared detector to measure the mass of carbon analysed. The ratio of FID signal generated per CO_2 formed (FID/CO_2) was shown to be strongly correlated ($R^2 = 0.89$) to the oxygen-to-carbon ratio (O/C) of the analyte. Furthermore, simple mixtures of analytes behaved as the weighted average of their components, indicating that this correlation extends to mixtures. These properties were also observed to correlate well with the sensitivity of the FID
20 estimated by structure activity relationships (quantified as the relative Effective Carbon Number). The relationships between measured FID/CO_2, analyte O/C, and FID sensitivity allow estimation of one property from another with <5% error for mixtures and <20% error for most individual analytes. The approach opens the possibility of field-deployable, autonomous measurement of the carbon and oxygen content of particulate matter using time-tested, low-maintenance detectors. Moreover, potential expansion to additional gas chromatography detectors may provide concurrent measurement of other
25 elements (e.g. sulphur, nitrogen).

1 Introduction

Atmospheric particulate matter, commonly referred to as aerosols, is responsible for a substantial fraction of annual global deaths (Dockery et al., 1993; Lim et al., 2012; World Health Organization, 2016) and is consequently monitored, primarily on a mass basis, throughout the world. A major fraction of these aerosols are comprised of organic compounds, which may
30 be directly emitted or form through the atmospheric oxidation of naturally and anthropogenically emitted volatile organic

compounds (Jimenez et al., 2009; Zhang et al., 2007). Owing to the wide range of sources and formation chemistry of aerosols, the composition may vary substantially, and differences in composition may affect the impacts of aerosols. In particular, the oxygen content of aerosols is a major driver of its impacts. For example, increased oxygenation increases hygroscopicity (Massoli et al., 2010), which increases cloud formation and impacts albedo (Intergovernmental Panel on
35   Climate Change, 2013) . Oxidized compounds are also more likely to fragment and volatilize upon further oxidation (Lambe et al., 2012). Furthermore, while aerosols are known to have deleterious effects, the "dose-response curve" that defines the increased risk of a given adverse health impact per unit exposure is poorly constrained (Apte et al., 2015; Burnett et al., 2014; Marshall et al., 2015). This uncertainty may be driven in part by observations that toxicity is compositionally dependent, with certain components of organic aerosol exhibiting higher toxicity than others (specifically: oxygenated
40   compounds (Tuet et al., 2016; Verma et al., 2015), oxidation products of biogenic gas-phase precursors (Kramer et al., 2016; Lin et al., 2016), and biomass burning emissions (Rohr and McDonald, 2016; Verma et al., 2015)). However, regulations and monitoring networks for aerosol mass typically do not include frequent or automated measurements of aerosol composition, limiting understanding of the physical, chemical, and physiological impacts of aerosols. New approaches are needed to facilitate low-maintenance measurements of aerosol composition, specifically with a focus on its oxygen content (e.g.,
45   oxygen-to-carbon ratio, O/C), which is a major driver of its health and climate impacts.

Currently, most widely used measurements of aerosol chemical composition use filter-based measurements, in which samples are collected for offline analyses conducted in a lab. Besides the time-integrated (multiple days or weeks) nature of the sampling, another drawback is the delay in the analysis, during which reaction or decomposition of the sample may occur. In contrast, real-time chemical composition data may be obtained with advanced mass spectrometric and/or
50   chromatographic instrumentation such as the Aerosol Mass Spectrometer (AMS), Aerosol Chemical Speciation Monitor (ACSM) (DeCarlo et al., 2006; Ng et al., 2011), or the Thermal-desorption Aerosol Gas chromatograph (TAG) (Williams et al., 2006). However, these instruments are difficult (though not impossible, (see (Budisulistiorini et al., 2013)) to deploy for long-term operation because of their high capital and operational costs, need for skilled operators, and complex data analysis. Due to these limitations, routine measurements of aerosols are primarily limited to quantification of their mass concentration.
55   A small amount of chemical information is available using moderate-cost instrumentation such as the OC/EC analyser (Sunset Labs), which separately quantifies elemental and organic carbon, but no tools are available to provide continuous measurement of the chemical composition of the organic component of aerosols despite the critical role it plays on aerosol impacts. Consequently, there remains a need for new methods that provide at least some chemical information about particle composition (e.g., O/C or other bulk chemical properties) without the need for mass spectrometry, chromatography, or other
60   high-cost or high-complexity techniques.

Moderate-cost robust measurement of aerosol carbon has been previously achieved using the operating principle of the flame ionization detector (FID), a common detector used in gas chromatography and previously implemented for particle measurements in OC/EC analysers. In an FID, analytes are combusted in a hydrogen flame, and signal is produced by electrometrically measuring ions (primarily CHO^+) produced by the flame (Holm, 1997, 1999). This approach has high

65   sensitivity, a large linear dynamic range (10^7), and robustness against variations in flow rates since FID is mass-sensitive rather than concentration-sensitive (Skoog et al., 2017). Most importantly, FID signal is nearly universal, with response proportional to the mass of carbon entering the detector. Addition of oxygenated functional groups decreases FID response, so current aerosol instrumentation relying on this detector typically catalytically convert all organic carbon to CO_2 and then CH_4, ensuring universal response to all aerosol carbon (Chow et al., 2001) . However, when molecular structures of analytes

70   are known, the FID sensitivity of an analyte can be calculated from established structure-activity relationships (Scanlon and Willis, 1985). Generally, , a carbon with a carbonyl does not produce any FID signal, and a carbon with a hydroxyl group produces half as much FID signal as a hydrocarbon. This relationship can be quantified more precisely as the Effective Carbon Number (ECN) of a compound, which describes FID response as equivalent to a hydrocarbon of a certain carbon number. Operating at ambient pressures and requiring only a source of hydrogen, the FID is consequently a stable and low-

75   cost alternative to mass spectrometry, providing robust quantification but with substantially reduced chemical resolution.

   Prior work has shown analytes to be combusted highly efficiently in an FID, even for highly oxygenated compounds (Fock, 1976) . This fact, coupled with the general trend that oxygenated functional groups decrease FID sensitivity, suggests that the simultaneous measurement of FID signal and the CO_2 produced in the flame should provide some estimate of oxygen content. In this work, we test this hypothesis by measuring the CO_2 produced by an FID using a non-dispersive infrared

80   absorption (NDIR) sensor. CO_2 detection by NDIR (specifically at wavelength 4.255 µm, wavenumber 2350 cm^{-1}) (LI-COR, 2007; Pandey and Kim, 2007) is widely used for continuous field measurements due to its accuracy and stability (Pandey and Kim, 2007). Simple implementation of this method requires only measurement of absolute absorption in a single optical cell, while more accurate (but complex) instruments may include a reference cell, with CO_2 measured from the differential absorption between the cells. This latter configuration finds more use in continuous monitoring instruments since any drift or

85   variation in beam strength can be accounted for with the reference measurement (Skoog et al., 1996). The high accuracy afforded by a two-cell approach (levels of detection of less than 100 ppb, (LI-COR, 2007) provides potential detection of FID-produced CO_2 at concentrations relevant to organic aerosol. For context, combustion of atmospherically-relevant concentrations of particles are expected to produce concentrations of CO_2 in the outflow of an FID of ~100 ppb to ~100 ppm using reasonable assumptions for a theoretical instrument based on this approach (see Supplementary Information for

90   calculation).

   In this work, we couple a CO_2 detector downstream of an FID to demonstrate a new approach to measure the carbon and oxygen content of atmospherically-relevant organic compounds. To provide a viable approach, three criteria need to be met:

     1) The FID must reproducibly (and ideally completely) combust all organic compounds, converting it to CO_2 for detection downstream to provide carbon mass.

95   2) FID response per carbon atom (i.e., measured ratio of signals, FID/CO_2) must be inversely proportional to the oxygen content of analytes and mixtures.

     3) One measurable parameter (e.g., FID/CO_2 signal ratios, analyte O/C, and analyte FID sensitivity) must predict any other to within reasonable error.

We systematically test these three criteria in this work, with the major goal of being able to predict any one parameter from
100 the others. While this work focuses on the theory and fundamental validation of the underlying approach, we discuss
potential applications to the study of atmospheric chemistry.

2 Materials and Methods

2.1 Theory of operation

Previous work has focused on quantifying the FID response of individual compounds, typically quantified as their Effective
105 Carbon Number (ECN). The ratio of this number to the number of carbons, N_C, in a compound is termed here the "relative
Effective Carbon Number" ($rECN = ECN/N_C$) and describes the average response of each carbon in a compound relative to
hydrocarbon response. The rECN can be thought of as the per-carbon FID sensitivity relative to the maximum possible.
Because oxygenated functional groups decrease FID response, the per-carbon FID sensitivity (i.e., rECN) necessarily
decreases with increasing oxygen content. The rate of this decrease is dependent on the structure of the oxygenated
110 functional groups because carbonyl and hydroxyl groups do not have equal effects on ECN. In Figure 1, the theoretical
slopes of compounds comprised solely of different functional groups are shown (dashed lines) as a function of O/C,
estimated from existing structure-activity relationships (Scanlon and Willis, 1985). Compounds entirely comprised of
carbonyls and carboxyls provide bounding cases, as the carbon atom in both groups produces no FID signal and they add one
and two oxygen atoms respectively; the slopes of these relationships are consequently rECN = -O/C and rECN = -0.5*O/C,
115 respectively. Compounds comprised only of alcohols fall in between, with a slope dependent somewhat on the specific
structures of the alcohols due to differences in the effects of primary, secondary, and tertiary alcohols (compounds used to
estimate slopes shown in Figure 1 are provided in Table S2 and Figure S1). ECNs for compounds spanning a range of
functionalities are available in published literature and are included in Figure 1. Nearly all compounds fall within the
bounding cases as expected, with an average slope approximately in the middle. These data suggest that a direct
120 measurement of rECN should reasonably describe the O/C of a compound.

2.2 Instrument description

A schematic of the instrument used to quantify the relationship between FID signal and CO_2 produced is shown in Figure 2a.
Individual analytes or mixtures were introduced to a thermally controlled cell from which they were thermally desorbed into
125 a helium carrier flow. Analytes were then transferred through heated transfer lines to the FID, using compressed CO_2-free
zero air as an oxygen source. For some configurations, an inline GC provided separation of analytes as discussed below. A
custom adapter was built to allow tubing to connect the FID outlet to the CO_2 detector. To prevent the water produced by the
FID hydrogen flame from impairing the carbon dioxide detector, the outflow of the FID was dried using an in-line Nafion
permeation dryer (MD-110-48F, Perma Pure LLC) with dry sheath air provided by a zero air generator used as dessicating

130   counterflow. The dried sample stream was detected by a NDIR CO_2 analyser (LI-6262 or LI-7000, LI-COR Biosciences), with CO_2 -free air provided to the reference cell. For all trials, helium served as the carrier and FID make-up gas where applicable. Theoretically, a flow split prior to the FID enables this configuration to be extended to additional detectors (e.g., flame photometric detector, nitrogen phosphorous detector) as shown in Figure 2a.

135   Three instrument configurations were used in order to analyse a wide range of compounds:

System 1: Aliquots of 0.2-1.0 µL of mixtures were injected into a heated inlet on a gas chromatograph (7890B, Agilent Technologies) and separated by gas chromatography (GC) on a non-polar column (Restek Rxi-5sil MS, 30 m x 0.25 mm x 0.25 um, temperature ramp of 6 °C/s from 40 to 310 °C). Analytes were detected by an on-board Agilent FID. For analysis of mixtures, parallel injections were performed on a GC coupled to a quadrupole mass spectrometer (GC-MS) as a detector

140   (7820A/5977, Agilent Technologies) for identification, with positive identification defined as match in the NIST mass spectral library with strength of at least 850, as well as a retention time in agreement with the retention indices published by NIST (Wallace, 2019). Identical columns and temperature ramps were used to allow identification based on retention time.

System 2: Solutions of individual analytes were injected into either a heated inlet (System 2a) or a room temperature passivated metal cell (System 2b). Aliquots of 0.2-1.0 µL individual organic compounds were injected at concentrations of

145   ~500 ng/uL in water or a carbonaceous solvent. Analytes were thermally desorbed and transferred through an inert guard column (Restek Hydroguard, 5m x 0.25 mm) isothermally heated (300 ºC) within the GC oven to the FID. Carbonaceous solvents were separated from the analyte by either the use of a cryotrap on System 2a or, for System 2b, desorbed at low temperature prior to higher-temperature desorption of the analyte. The cryotrap was situated on the transfer line within the oven and cooled by liquid nitrogen to a temperature that trapped the analyte but not solvent, then heated to volatilize the

150   analyte of interest.

System 3: Individual analytes were injected into a room temperature passivated metal cell as above. Solvent was allowed to evolve at slightly elevated temperatures, then the analyte was thermally desorbed with 20 sccm helium through a custom isothermally heated (250º C) transfer line directly to the FID. On this system the FID used was from Scientific Research Instruments (SRI) on a Model 110 Detector Chassis, with signals recorded using a custom Labview program (National

155   Instruments).

System 1 allowed concurrent analysis of multiple analytes from commercially available mixtures to facilitate analysis of large numbers of analytes but was limited in its application of highly oxygenated compounds due to their inability to elute from a GC column. System 2 addressed this limitation by permitting injection of aqueous solutions of more oxygenated compounds that could not elute through the GC. System 3 is functionally similar to System 2b but approaches the

160   configuration of a potentially field-deployable instrument. On each system, a mixture of *n*-alkanes was used to provide hydrocarbon response of the FID on each day of experiments (C_7-C_{40}, Supelco), as well as correct for differences in retention times between systems. The metal desorption cell used in Systems 2b and 3 was identical to that previously described for use with the field-deployable Thermal desorption Aerosol Gas chromatograph (TAG) (Kreisberg et al., 2009) .

Sample data from System 1 is shown in Figure 2b. FID response and CO_2 response are closely coupled, with a delay in the
165   CO_2 signal of 3-5 seconds due to transit time through the permeation dryer. Resolution on the CO_2 channel is slightly
degraded due to band broadening during this transit, but chromatographic peaks are nevertheless clear. Concentrations of
CO_2 in the flow are only on the order of 1 ppm per 10 ng of analyte, resulting in the relatively low observed signal-to-noise
on this channel.

170   **2.3 Materials**

A variety of mixtures and individual compounds were analysed in this work. Mixtures of unknown analytes included
commercially available products obtained from a local grocery store, including four scents of air freshener and six perfumes
and colognes. Dilutions of all fragrances were made in methylene chloride (DCM) solvent (1-10% v/v). Aqueous solutions
of oxygenated analytes were made with deionized water produced by a Barnstead/Thermolyne NANOpure Analytical
175   Deionization System, Model D4744. Individuals compounds analysed were provided by Sigma-Aldrich, Acros Organics,
Fisher Scientific, Alfa Aesar, and Fluka, all at purities of at least 98%.

2.4 Experimental details

Systems 1 and 2 provided data for ~90 analytes, from which the ratio of FID signal/CO_2 signal (FID response per CO_2
180   produced) versus O/C ratio could be plotted. Individual compounds were injected at concentrations of approximately 250
ng/µL, either as aqueous solutions or in a carbonaceous solvent purged prior to thermal desorption as described. In all cases,
FID/CO_2 of oxygenated and unsaturated compounds were normalized to the FID/CO_2 ratio of the *n*-alkane with the nearest
retention time to determine the FID response. This approach provides a value of 1 unit of FID response per CO_2 produced for
n-alkanes (which have the maximum possible FID response), and a value less than or equal to 1 for any other components.
185   System 3 was used to corroborate results from Systems 1 and 2 in a configuration closer to that expected for field-deployable
instrumentation. It was also used to measure combustion efficiency of the FID and analyse multi-component mixtures. To
assess combustion efficiency, a known mass flow of CO_2 gas (2 sccm of 1% CO_2 in balance air) was introduced to the
desorption cell in the same location as the injection of analytes to provide signal-to-mass response factor for the CO_2
analyser. Mass of carbon introduced as an analyte was compared to mass of CO_2 detected. Four analytes were tested for
190   complete combustion spanning the range of O/C as described in Section 3. For analysis of multi-component mixtures,
individual analytes were combined into solution at varying relative concentrations. Components were selected with differing
O/C ratios to provide large changes in FID response, but similar vapor pressures, p^0, to ensure both analytes were desorbed
together and reached the FID and CO_2 analyser at approximately the same time. The four compounds used to meet these
requirements were: dodecane, p^0 = 18 Pa, O/C = 0; 1-octanol, p^0 = 11 Pa, O/C = 0.125; hydroxyethyl methacrylate, p^0 = 17

Pa, O/C = 0.5; and propylene glycol, p^0 = 17 Pa, O/C = 0.66 (vapor pressures from EPI Suite software values at 25°C, (US
EPA, 2019)).

For comparison of measured data to ECN, estimated ECN was calculated based on the criteria of Scanlon (Scanlon and
Willis, 1985). ECN for compounds with multiple functional groups were determined based on different literature (Jorgensen,
1990). Relative ECN is calculated as the ratio of this estimated ECN to the number of carbon atoms in the analyte.

200 Chromatographic peaks and thermograms were analysed and integrated using the publicly available TERN software package
(Isaacman-VanWertz et al., 2017) in the Igor Pro programming environment (Wavemetrics, Inc.). For data with replicate
measurements, potential outliers were discarded based on Dixon's Q test with a 95% confidence level.

3 Results and Discussion

3.1 Complete combustion by FID

205 Quantification of CO_2 produced from the analysis of known amounts of analytes provides an estimate of the efficiency of the
conversion from organic carbon to CO_2 in the FID. Figure 3 depicts the results for four different analytes of varying degrees
of oxygenation, along with a 1:1 line for reference. The average conversion of all analytes is ~95%, indicating nearly
complete combustion. Less oxygenated analytes (squalene and diethyl phthalate, introduced as solutions in DCM) exhibited
efficient conversion with highly reproducible results: 95% conversion and a relative standard deviation (RSD) between

210 replicate injections of ~5%. More oxygenated components, which were introduced as aqueous solutions, were more variable.
Hydroxyethyl methacrylate ("HEM") had a mean conversion of 100%, but with a somewhat more variable RSD of 13%.
Propylene glycol had a mean yield of only 87% and an RSD of 7%. These differences may be explained in part by solvent
effects. The DCM could be evolved entirely before heating the cell, yielding higher precision for squalene and diethyl
phthalate trials. However, solvent blanks of water gave small signals on the CO_2 detector and corrections were made to the

215 HEM and propylene glycol peaks. As concentrations of HEM and propylene glycol became more dilute, the background
water signal became comparatively large and uncertainty grew. Overall, however, the four compounds showed strong
linearity and high percentage yields, supporting the conclusion that the CO_2 detector accurately measures total carbon.

3.2 Correlation between measured variables

220 Figure 4 shows correlations between three parameters: FID/CO_2 signals, estimated relative ECN, and O/C. FID/CO_2, the
amount of FID signal generated per CO_2 produced relative to n-alkanes, correlates closely with O/C (Figure 4a, R^2 = 0.89
and slope = -0.54). This measured parameter is theoretically equivalent to the amount of FID signal generated per carbon
atom relative to n-alkanes, which is the definition of rECN. This observation, and the comparison between rECN and O/C
shown for literature data in Figure 1 suggests that rECN should equal the measured FID/CO_2, which are indeed observed to

225 correlate closely (Figure 4b). FID/CO_2 tends to be slightly lower than expected, which is likely due in part to uncertainty in

structure-activity based estimation of ECN, which has been previously shown even for hydrocarbons to be on the order of 10% with a tendency to overestimate (Faiola et al., 2012) . Close correlations between FID/CO_2 and both rECN and O/C indicate that rECN and O/C must also be correlated, which is shown to be true in Figure 4c. Uncertainty in the average trends of these relationships is very low, with uncertainty in the slopes of less than 4% in all cases. For 14 of the analytes

230   shown, FID/CO_2 was measured in more than one instrument configuration, with results from one configuration always within 7% of the average value for an analyte (Figure S2). FID/CO_2 is therefore largely independent on the mechanism by which an analyte was thermally transferred, and uncertainty in the measured FID/CO_2 of an individual component is on the order of 10%.

Comparison of Figures 1 and 4c shows that the fitted slope of rECN versus O/C falls well within the boundaries demarcated

235   by the carbonyls and carboxyl groups, -1.0 and -0.5, respectively, and that the compounds used in this work follow the same trends as previously published ECN data. It is notable but probably incidental that the observed downward slopes and R^2 values match closely with those of a set of alcohols, -0.58. Methanol (open symbol in Figure 4) is an apparent outlier and excluded in these fits because it may be attributable to a unique feature of methanol combustion in an FID. During pre-combustion in the hot hydrogen-rich environment of the FID, multicarbon alcohols lose water through elimination to form an

240   alkene, a pathway that is significant for larger alcohols but is not available to methanol (Holm, 1997). We speculate therefore that methanol falls off the line as it undergoes a fundamentally different combustion process than all other alcohols, so its behaviour as an outlier does not have negative implications for the application of this system to larger compounds.

In order to be useful in the analysis of atmospheric particles, the observed relationships between O/C and other parameters must hold for mixtures as well as individual analytes. To test this requirement, mixtures were analysed comprised of varying

245   fractions of two components. Results from three separate mixtures containing two of these components at a time are shown in Figure 5. The expected FID/CO_2 was calculated as the average of the two pure components weighted by their carbon fraction in the mixture. The measured FID/CO_2 was the experimental value of the mixture. An orthogonal linear fit of the three tested mixtures (each at seven varying relative fractions of each component) shows a slope of 0.95. The deviation of the Figure 5 slope from unity may be due to uncertainties in the measured FID/CO_2 ratios of single components used in the

250   weighted average calculation of the expected ratio, since comparison between instrument configurations suggests uncertainties of ~10% in any individually measure FID/CO_2. Overall, the observed FID/CO_2 ratios of mixtures correspond quite well with the expected ratios across the full range of anticipated measurements, demonstrating that the FID/CO_2 ratios observed for single components are maintained in mixtures.

255   **3.3 Error estimates**

The major benefit of quantifying the relationships between O/C, rECN, and measured FID/CO_2 is their potential use in predicting one parameter from another. A sufficiently complex mixture should approximate the central tendencies of the relationships, and the average trends in these relationships have low uncertainty (<5% uncertainty in slopes). The application

of this approach to complex mixtures (e.g., organic aerosols) is therefore expected to have low (5-10%) uncertainty.
260 However, in other cases, these relationships may be useful for the prediction of an unknown parameter of an individual analyte, which necessarily leads to higher error.

To assess the accuracy in calculating unknown variables from observed values for individual analytes, absolute and relative (%) errors are shown in Figure 6. Error in predicted values is less than 20% in nearly all cases, but it is often much lower and exhibits some heteroscedasticity worth discussing. Generally, absolute error is higher for oxygenated components due to the
265 structurally-dependent effects of oxygen, which are ignored in these relationships (e.g., the divergence of the carbonyl and carboxyl trends). However, prediction of O/C from FID/CO_2 yields very high relative error despite low absolute error at low O/C because as O/C approaches 0, even low absolute errors imply high relative error. For highly oxygenated compounds, relative error in O/C appears to plateau to about 20%. Error in this relationship can be reasonably summarized as a relative error of 20% with a minimum absolute error of approximately 0.05. Generally, the rECN can be predicted from either
270 FID/CO_2 (Figure 6b) or O/C (Figure 6c) with errors of 10-15% for highly oxygenated compounds, and <5% for less oxygenated compounds (O/C < ~0.5). These low errors indicate that the sensitivity of an FID can be estimated with high certainty either directly from O/C or, in the absence of this information, from a direct measurement of FID/CO_2.

4 Conclusions and Applications

275 This work demonstrates that the carbon and oxygen content of single compounds and mixtures can be directly measured by coupling an FID and a downstream CO_2 analyser. Specifically, three major conclusions support this claim:

1. Nearly complete combustion (~95%) in an FID of a wide range of organic compounds allows direct quantification of analysed carbon as the amount of CO_2 produced
2. Oxygen content (as O/C) is closely correlated with the amount of FID signal produced per CO_2 generated
280 (FID/CO_2), as well as existing structure-activity estimates of per-carbon FID sensitivity (rECN). These correlations extend to multi-component mixtures.
3. Uncertainties in the average trends between these parameters are less than 5%, and in the prediction of an unknown parameter from a known parameter are <20%.

The correlations between O/C, FID/CO_2, and rECN quantified in this work may advance the field of atmospheric chemistry
285 through a variety of possible applications we consider here:

- The instrumental set-up described in this work could be implemented as a field-deployable tool for measurement of carbon and oxygen content of particles. Such an instrument would be more robust and lower maintenance than currently available instrumentation for the automated characterization of aerosol chemical composition, though would also provide lower chemical detail compared to mass spectrometric instrumentation. However, it could
290 provide O/C, an important parameter for aerosol chemical modelling and understanding aerosol impacts. Moreover,

the use of GC detectors as an instrument platform allows potential inclusion to additional of other detectors (e.g. FPD for sulphur or phosphorus, NPD for nitrogen or phosphorus) permitting a more comprehensive view of the chemical composition of aerosols. The compounds used to develop the relationships in this work may not reflect the average composition of ambient aerosols, which may contain functional groups not represented here (e.g., peroxides, nitrates, etc.). Application of the demonstrated relationships in an atmospheric context would consequently require some comparison with currently accepted approaches to measure O/C, but the general trends shown in this work are sufficiently robust to provide some insight into atmospheric composition.

- An FID could be used as a calibration tool for new instrumentation. While the FID is an attractive near-universal detector, the structural dependence of its response has limited its adoption. However, we demonstrate here that FID sensitivity can be robustly estimated with low uncertainty from O/C or measured FID/CO_2 ratio. This implies that any instrument that can be coupled to an FID can use it for quantification, regardless of whether a molecular formula is available. For instruments that do provide a molecular formula (e.g., chemical ionization mass spectrometers), quantification by FID is possible even without including the additional complexity of a CO_2 analyser. Signal from a novel instrument could be combined with quantification by FID to estimate instrument sensitivity.

- A CO_2 analyser could provide an additional dimension of chemical resolution for an FID being used as a GC detector. For example, identification of an analyte by its retention time could be confirmed by its FID/CO_2 ratio.

These possible applications provide a demonstration of the utility of the novel approach presented here. Quantifying the average relationships between FID sensitivity, O/C, and a directly measurable parameter opens the door to a wide range of potential new moderate cost measurement techniques that may find use in the field.

Acknowledgements

This work was supported through the Department of Energy SBIR/STTR Program, grant number DE-SC0018462.

References

Apte, J. S., Marshall, J. D., Cohen, A. J. and Brauer, M.: Addressing Global Mortality from Ambient PM 2.5, Environ. Sci. Technol., 49, 8057–8066, doi:10.1021/acs.est.5b01236, 2015.

Budisulistiorini, S. H., Canagaratna, M. R., Croteau, P. L., Marth, W. J., Baumann, K., Edgerton, E. S., Shaw, S. L., Knipping, E. M., Worsnop, D. R., Jayne, J. T., Gold, A. and Surratt, J. D.: Real-time continuous characterization of secondary organic aerosol derived from isoprene epoxydiols in downtown Atlanta, Georgia, using the aerodyne aerosol chemical speciation monitor, Environ. Sci. Technol., 47(11), 5686–5694, doi:10.1021/es400023n, 2013.

Burnett, R. T., III, C. A. P., Ezzati, M., Olives, C., Lim, S. S. and Mehta, S.: An Integrated Risk Function for Estimating the Global Burden of Disease Attributable to Ambient Fine Particulate Matter Exposure, Environ. Health Perspect., 122(4), 397–404, doi:10.1289/ehp.1307049, 2014.

325

Chow, J. C., Watson, J. G., Crow, D., Lowenthal, D. H., Chow, J. C., Watson, J. G., Crow, D., Lowenthal, D. H., Chow, J. C., Watson, J. G., Crow, D., Lowenthal, D. H. and Merri, T.: Comparison of IMPROVE and NIOSH Carbon Measurements Comparison of IMPROVE and NIOSH Carbon Measurements, Aerosol Sci. Technol., 34, 23–34, doi:10.1080/02786820119073, 2001.

330

DeCarlo, P. F., Kimmel, J. R., Trimborn, A., Northway, M. J., Jayne, J. T., Aiken, A. C., Gonin, M., Fuhrer, K., Horvath, T., Docherty, K. S., Worsnop, D. R. and Jimenez, J. L.: Field-deployable, high-resolution, time-of-flight aerosol mass spectrometer, Anal. Chem., 78(24), 8281–8289, doi:10.1021/ac061249n, 2006.

335 Dockery, D. W., Pope III, C. A., Xu, X., Spengler, J. D., Ware, J. H., Fay, M. E., Ferris Jr, B. G. and Speizer, F. E.: An Associaton between Air Pollution and Mortality in Six U.S. Cities, N. Engl. J. Med., 330(2), 141, doi:101056/NEJM199312093292401, 1993.

Faiola, C. L., Erickson, M. H., Fricaud, V. L., Jobson, B. T. and Vanreken, T. M.: Quantification of biogenic volatile organic
340 compounds with a flame ionization detector using the effective carbon number concept, Atmos. Meas. Tech., 5(8), 1911–1923, doi:10.5194/amt-5-1911-2012, 2012.

Fock, H.: Radio Gas Chromatography of 14C-Labelled Compounds by Measuring the Radioactivity of the FID Combustion Products After G LC Analysis, Chromatographia, 9(3), 99–104, doi:10.1007/BF02330375, 1976.

345

Holm, T.: Mechanism of the flame ionization detector II. Isotope effects and heteroatom effects, J. Chromatogr. A, 782, 81–86, doi:10.1016/S0021-9673(98)00706-7, 1997.

Holm, T.: Aspects of the mechanism of the flame ionization detector, J. Chromatogr. A, 842, 221–227, doi:10.1016/S0021-
350 9673(98)00706-7, 1999.

Intergovernmental Panel on Climate Change: Climate Change 2013: The Physical Science Basis. Contribution of Working Group I to the Fifth Assessment Report of the Intergovern- mental Panel on Climate Change, edited by T. F. Stocker, D. Qin, G.-K. Plattner, M. Tignor, S. K. Allen, J. Boschung, A. Nauels, Y. Xia, V. Bex, and P. M. Midgley, Cambridge University

355   Press, Cambridge, United Kingdom and New York, NY, USA., 2013.

Isaacman-VanWertz, G., Sueper, D. T., Aikin, K. C., Lerner, B. M., Gilman, J. B., de Gouw, J. A., Worsnop, D. R. and Goldstein, A. H.: Automated single-ion peak fitting as an efficient approach for analyzing complex chromatographic data, J. Chromatogr. A, 1529, 81–92, doi:10.1016/j.chroma.2017.11.005, 2017.

360

Jimenez, J. L., Canagaratna, M. R., Donahue, N. M., Prevot, A. S. H., Zhang, Q., Kroll, J. H., Decarlo, P. F., Allan, J. D., Coe, H., Ng, N. L., Aiken, A. C., Ulbrich, I. M., Grieshop, A. P., Duplissy, J., Wilson, K. R., Lanz, V. A., Hueglin, C., Sun, Y. L., Tian, J., Laaksonen, A., Raatikainen, T., Rautiainen, J., Vaattovaara, P., Ehn, M., Kulmala, M., Tomlinson, J. M., Cubison, M. J., Dunlea, E. J., Alfarra, M. R., Williams, P. I., Bower, K., Kondo, Y., Schneider, J., Drewnick, F., Borrmann, 365 S., Weimer, S., Demerjian, K., Salcedo, D., Cottrell, L., Takami, A., Miyoshi, T., Shimono, A., Sun, J. Y., Zhang, Y. M., Dzepina, K., Sueper, D., Jayne, J. T., Herndon, S. C., Williams, L. R., Wood, E. C., Middlebrook, A. M., Kolb, C. E., Baltensperger, U. and Worsnop, D. R.: Evolution of Organic Aerosols in the Atmosphere, Science (80-.)., 326(December), 1525–1530, doi:10.1126/science.1180353, 2009.

370   Jorgensen, A. D.: Prediction of Gas Chromatography Flame Ionization Detector Response Factors from Molecular Structures, Anal. Chem., 62(7), 683–689, doi:10.1021/ac00206a007, 1990.

Kramer, A. J., Rattanavaraha, W., Zhang, Z., Gold, A., Surratt, J. D. and Lin, Y.: Assessing the oxidative potential of isoprene-derived epoxides and secondary organic aerosol, Atmos. Environ., 130, 211–218, 375   doi:10.1016/j.atmosenv.2015.10.018, 2016.

Kreisberg, N. M., Hering, S. V., Williams, B. J., Williams, B. J., Worton, D. R. and Goldstein, A. H.: Quantification of hourly speciated organic compounds in atmospheric aerosols, measured by an in-situ thermal desorption aerosol gas chromatograph (tag), Aerosol Sci. Technol., 43(1), 38–52, doi:10.1080/02786820802459583, 2009.

380

Lambe, A. T., Onasch, T. B., Croasdale, D. R., Wright, J. P., Martin, A. T., Franklin, J. P., Massoli, P., Kroll, J. H., Canagaratna, M. R., Brune, W. H., Worsnop, D. R. and Davidovits, P.: Transitions from Functionalization to Fragmentation Reactions of Laboratory Secondary Organic Aerosol (SOA) Generated from the OH Oxidation of Alkane Precursors, Environ. Sci. Technol., 46, 5430–5437, doi:10.1021/es300274t, 2012.

385

LI-COR, I.: LI-7000 Instruction Manual, LI-COR,Inc., Lincoln, NE 68504., 2007.

Lim, S. S., Vos, T., Flaxman, A. D., Danaei, G., Shibuya, K., Adair-Rohani, H., Amann, M., Anderson, H. R., Andrews, K.

G., Aryee, M., Atkinson, C., Bacchus, L. J., Bahalim, A. N., Balakrishnan, K., Balmes, J., Barker-Collo, S., Baxter, A., Bell,
390 M. L., Blore, J. D., Blyth, F., Bonner, C., Borges, G., Bourne, R., Boussinesq, M., Brauer, M., Brooks, P., Bruce, N. G.,
Brunekreef, B., Bryan-Hancock, C., Bucello, C., Buchbinder, R., Bull, F., Burnett, R. T., Byers, T. E., Calabria, B.,
Carapetis, J., Carnahan, E., Chafe, Z., Charlson, F., Chen, H., Chen, J. S., Cheng, A. T. A., Child, J. C., Cohen, A., Colson,
K. E., Cowie, B. C., Darby, S., Darling, S., Davis, A., Degenhardt, L., Dentener, F., Des Jarlais, D. C., Devries, K., Dherani,
M., Ding, E. L., Dorsey, E. R., Driscoll, T., Edmond, K., Ali, S. E., Engell, R. E., Erwin, P. J., Fahimi, S., Falder, G.,
395 Farzadfar, F., Ferrari, A., Finucane, M. M., Flaxman, S., Fowkes, F. G. R., Freedman, G., Freeman, M. K., Gakidou, E.,
Ghosh, S., Giovannucci, E., Gmel, G., Graham, K., Grainger, R., Grant, B., Gunnell, D., Gutierrez, H. R., Hall, W., Hoek, H.
W., Hogan, A., Hosgood, H. D., Hoy, D., Hu, H., Hubbell, B. J., Hutchings, S. J., Ibeanusi, S. E., Jacklyn, G. L., Jasrasaria,
R., Jonas, J. B., Kan, H., Kanis, J. A., Kassebaum, N., Kawakami, N., Khang, Y. H., Khatibzadeh, S., Khoo, J. P., Kok, C., et
al.: A comparative risk assessment of burden of disease and injury attributable to 67 risk factors and risk factor clusters in 21
400 regions, 1990-2010: A systematic analysis for the Global Burden of Disease Study 2010, Lancet, 380(9859), 2224–2260,
doi:10.1016/S0140-6736(12)61766-8, 2012.

Lin, Y. H., Arashiro, M., Martin, E., Chen, Y., Zhang, Z., Sexton, K. G., Gold, A., Jaspers, I., Fry, R. C. and Surratt, J. D.:
Isoprene-derived secondary organic aerosol induces the expression of oxidative stress response genes in human lung cells,
405 Environ. Sci. Technol. Lett., 3(6), 250–254, doi:10.1021/acs.estlett.6b00151, 2016.

Marshall, J. D., Apte, J. S., Coggins, J. S. and Goodkind, A. L.: Blue Skies Bluer ?, Environ. Sci. Technol., 49, 13929–
13936, doi:10.1021/acs.est.5b03154, 2015.

410 Massoli, P., Lambe, A. T., Ahern, A. T., Williams, L. R., Ehn, M., Mikkilä, J., Canagaratna, M. R., Brune, W. H., Onasch,
T. B., Jayne, J. T., Petäjä, T., Kulmala, M., Laaksonen, A., Kolb, C. E., Davidovits, P. and Worsnop, D. R.: Relationship
between aerosol oxidation level and hygroscopic properties of laboratory generated secondary organic aerosol (SOA)
particles, Geophys. Res. Lett., 37(L24801), 1–5, doi:10.1029/2010GL045258, 2010.

415 Ng, N. L., Herndon, S. C., Trimborn, A., Canagaratna, M. R., Croteau, P. L., Onasch, T. B., Sueper, D., Worsnop, D. R.,
Zhang, Q., Sun, Y. L. and Jayne, J. T.: An Aerosol Chemical Speciation Monitor (ACSM) for routine monitoring of the
composition and mass concentrations of ambient aerosol, Aerosol Sci. Technol., 45(7), 770–784,
doi:10.1080/02786826.2011.560211, 2011.

420 Pandey, S. K. and Kim, K. H.: The relative performance of NDIR-based sensors in the near real-time analysis of CO2 in air,
Sensors, 7(9), 1683–1696, doi:10.3390/s7091683, 2007.

Rohr, A. and McDonald, J.: Health effects of carbon-containing particulate matter : focus on sources and recent research program results, Crit. Rev. Toxicol., 46(2), 97–137, doi:10.3109/10408444.2015.1107024, 2016.

425

Scanlon, J. T. and Willis, D. E.: Calculation using effective carbon number, J. Chromatogr. Sci., 23, 333–340, doi:10.1093/chromsci/23.8.333, 1985.

Skoog, D. A., West, D. M. and Holler, J. F.: Fun

430   damentals of Analytical Chemistry , 7th Edition, Saunders College Publishing, Philadelphia, PA 19106-3412., 1996.

Skoog, D. A., Holler, J. F. and Crouch, S. R.: Principles of Instrumental Analysis, Cengage Learning, Boston, MA 02210., 2017.

435   Tuet, W. Y., Fok, S., Verma, V., Tagle, M. S., Grosberg, A., Champion, J. A., Ng, N. L. and Rns, R. O. S.: Dose-dependent intracellular reactive oxygen and nitrogen species (ROS/RNS) production from particulate matter exposure : comparison to oxidative potential and chemical composition, Atmos. Environ., 144, 335–344, doi:10.1016/j.atmosenv.2016.09.005, 2016.

US EPA: Estimation Programs Interface Suite for Microsoft Windows, 2019.

440

Verma, V., Wang, Y., El-a, R., Fang, T., Rowland, J., Russell, A. G. and Weber, R. J.: Fractionating ambient humic-like substances (HULIS) for their reactive oxygen species activity e Assessing the importance of quinones and atmospheric aging, Atmos. Environ., 120, 351–359, doi:10.1016/j.atmosenv.2015.09.010, 2015.

445   Wallace, W. E.: Mass Spectra, in NIST Chemistry WebBook, NIST Standard Reference Database, Number 69, edited by P. J. Linstrom and W. G. Mallard, National Institute of Standards and Technology, Gaithersburg, MD 20899., 2019.
Williams, B., Goldstein, A., Kreisberg, N. and Hering, S.: An in-situ instrument for speciated organic composition of atmospheric aerosols: Thermal desorption aerosol GC/MS-FID (TAG), Aerosol Sci. Technol., 40(8), 627–638, doi:10.1080/02786820600754631, 2006.

450

World Health Organization: Ambient air pollution: a global assessment of exposure and burden of disease. [online] Available from: https://apps.who.int/iris/bitstream/handle/10665/250141/9789241511353-eng.pdf?sequence=1, 2016.

Zhang, Q., Jimenez, J. L., Canagaratna, M. R., Allan, J. D., Coe, H., Ulbrich, I., Alfarra, M. R., Takami, A., Middlebrook, A.

455   M., Sun, Y. L., Dzepina, K., Dunlea, E., Docherty, K., Decarlo, P. F., Salcedo, D., Onasch, T., Jayne, J. T., Miyoshi, T., Shimono, A., Hatakeyama, S., Takegawa, N., Kondo, Y., Schneider, J., Drewnick, F., Cottrell, L., Griffin, R. J., Rautiainen,

J., Sun, J. Y. and Zhang, Y. M.: Ubiquity and dominance of oxygenated species in organic aerosols in anthropogenically-influenced Northern Hemisphere midlatitudes, Geophys. Res. Lett., 34(L13801), 1–6, doi:10.1029/2007GL029979, 2007.

460
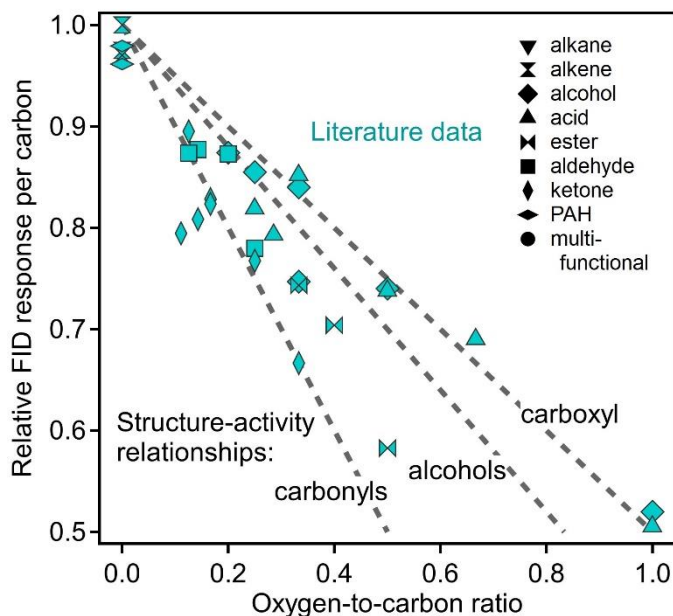
Figure 1: Plot of relative ECN versus O/C ratios based on literature values. Literature data are from Scanlon and Willis (1985), representing a variety of functional groups shown as different shapes. Dashed lines are the theoretical slopes of compounds comprised completely of labelled functional groups, based on the structure-activity relationship provided by Scanlon and Willis
465 **(1985). Compounds used to develop these slopes are provided in Table S2.**
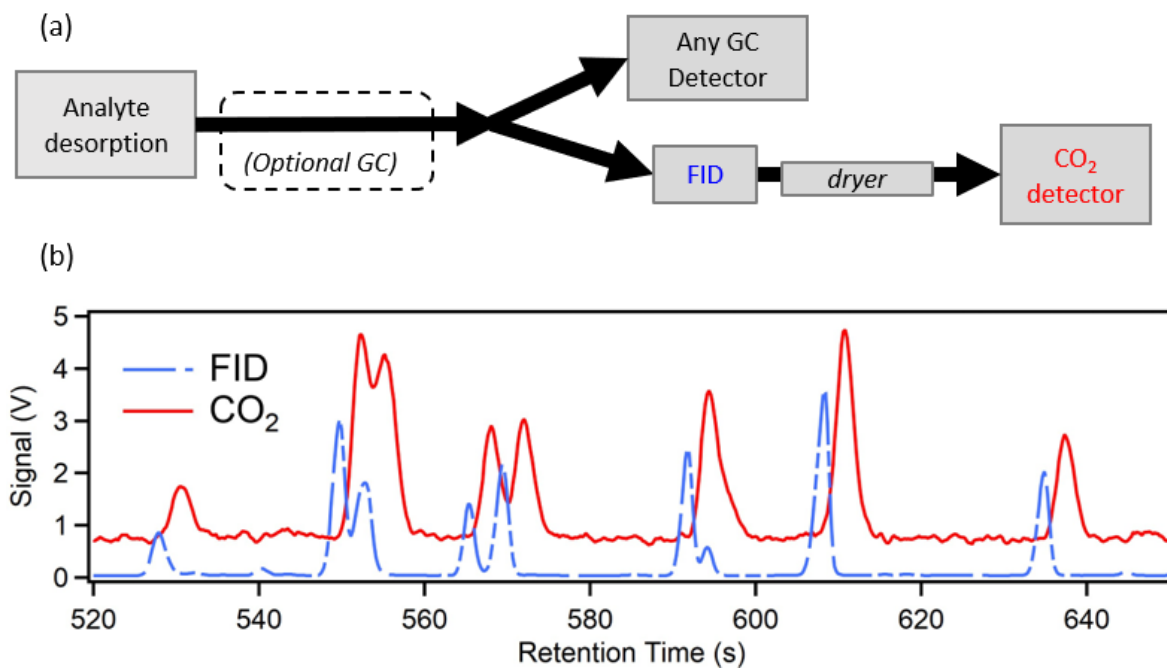
Figure 2: (a) A generalized schematic of the instrument configurations. Optional GC was used for System 1 only. (b) Sample data of simultaneously measured FID and CO_2 signals.
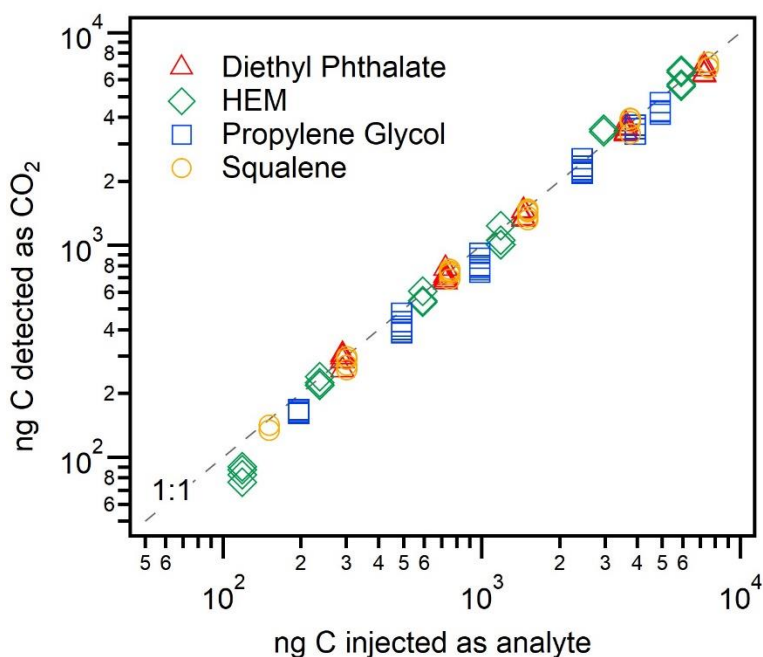
Figure 3: FID combustion efficiency, shown as ng of carbon measured by the CO_2 detector versus ng C injected as one of four analytes: squalene ($C_{30}H_{50}$), diethyl phthalate ($C_{12}H_{14}O_4$), hydroxyethyl methacrylate ($C_6H_{10}O_3$) and propylene glycol ($C_3H_8O_2$).

475
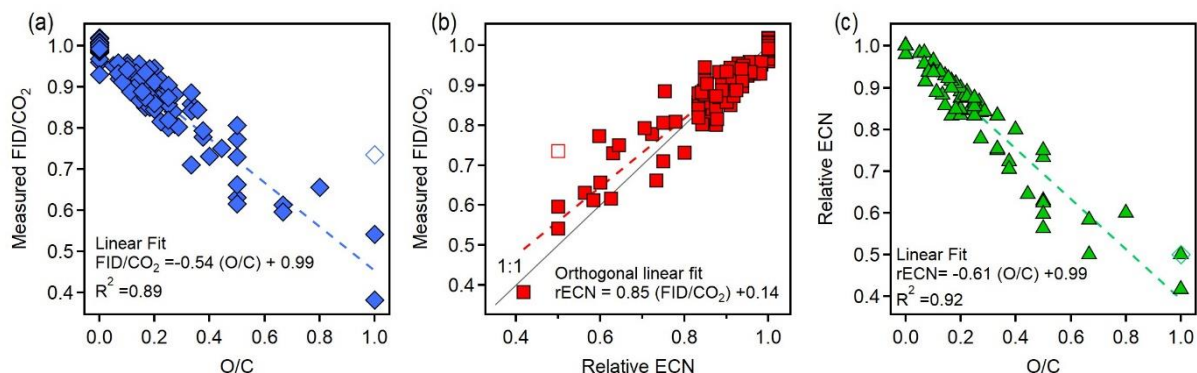
Figure 4: Plots relating the three variables: measured FID/CO₂ relative to *n*-alkanes, relative ECN, and O/C. Comparisons shown are (a) FID/CO₂ versus O/C, (b) FID/CO₂ versus relative ECN, and (c) relative ECN versus O/C. Dashed lines are linear fits; fits assume error only in dependent variable in the case of comparisons to O/C (which has no error), and assume error in both variables ("orthogonal fit") in the case of rECN comparison to FID/CO₂. Methanol is shown in each plot as an unfilled marker as there are physical reasons it may be an outlier (discussed in the main text).
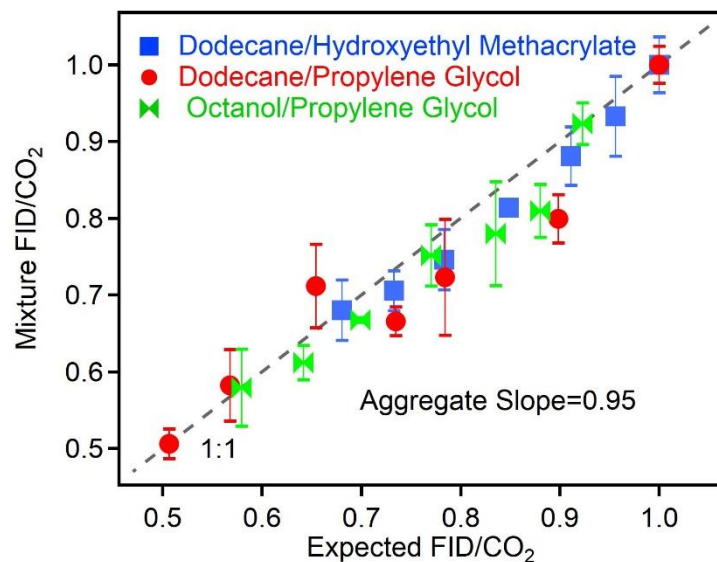
Figure 5: Measured FID/CO₂ of mixtures compare to the expected FID/CO₂ based on the weighted carbon fraction of the individual components. Each point represents the average of 3-5 replicates, with relative standard deviations of less than 10%. Dashed line shows 1:1 line.
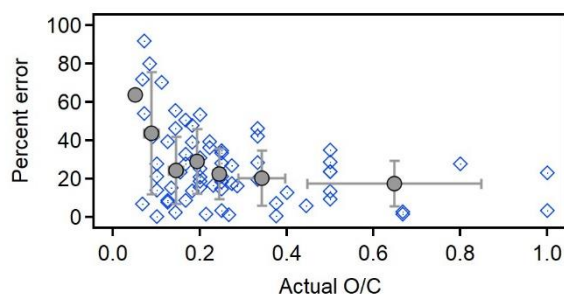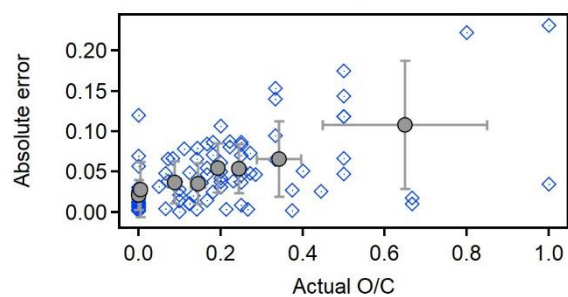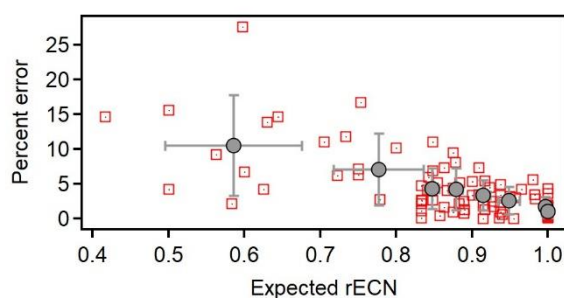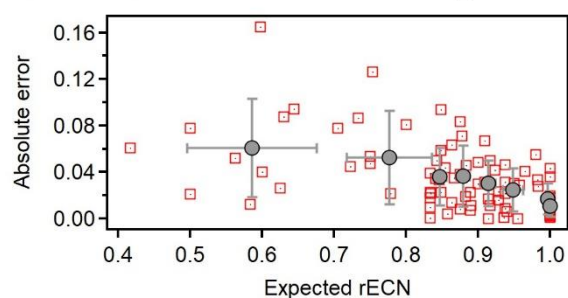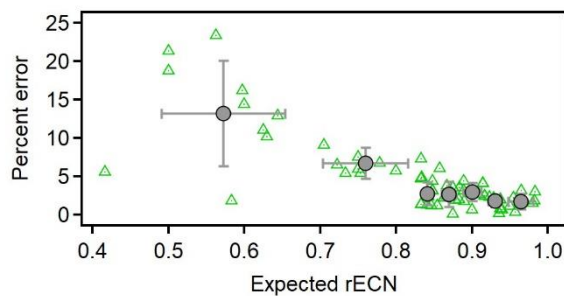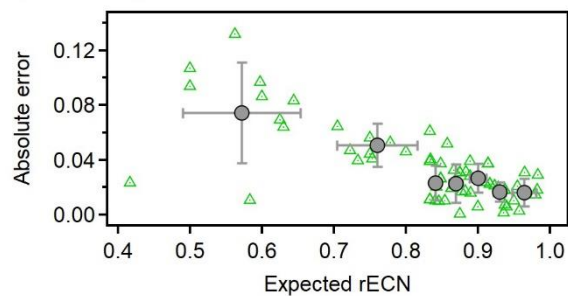
490   **Figure 6: Absolute error (left panels) and relative error (right panels) in the prediction of (a) O/C from FID/CO₂, (b) rECN from FID/CO₂ (c) rECN from O/C. All errors shown against the actual value of the predicted value (i.e., compound O/C, or rECN estimated from structure-activity relationships). Relative error calculated as |observed-actual|/actual*100%. All analysed compounds (N=89) shown as individual points with the same colours and shapes as Figure 3. To make trends more qualitatively clear quantiles of equal number of points are shown in grey (quantile average with standard deviation as error bar).**

495